



Title	Composition and Structure Changes in Al ₃ Ni ₂ Microchannel Lining Layers by Alkali Leaching
Author(s)	Saitoh, Yusuke; Ohmi, Tatsuya; Sakairi, Masatoshi; Kumagai, Takehiko; Iguchi, Manabu
Citation	実験力学, 12(Special Issue), s237-s242 https://doi.org/10.11395/jjsem.12.s237
Issue Date	2012-07-01
Doc URL	http://hdl.handle.net/2115/74645
Rights	著作権は日本実験力学学会にある。利用は著作権の範囲内に限られる。
Type	article
File Information	vol.12 s237- JSEM..pdf



[Instructions for use](#)

Composition and Structure Changes in Al₃Ni₂ Microchannel Lining Layers by Alkali Leaching

Yusuke SAITOH¹, Tatsuya OHMI², Masatoshi SAKAIRI², Takehiko KUMAGAI² and Manabu IGUCHI²

¹ Graduate School of Engineering, Hokkaido University, Sapporo, Hokkaido, 060-8628, Japan

² Faculty of Engineering, Hokkaido University, Sapporo, Hokkaido, 060-8628, Japan

(Received 10 December 2011; received in revised form 16 March 2012; accepted 26 April 2012)

Abstract

Effects of alkali leaching time on the composition and structure changes in the Al₃Ni₂ microchannel lining layer produced by a sacrificial-core method have been investigated. The composition was measured both on the specimen surface directly exposed to the leachant and on the new surface cut after alkali leaching. In each surface, the decrease in Al concentration became sluggish after formation of Ni₃Al. On the other hand, nano structure consisted of almost pure Ni was detected on the inner wall of the microchannel leached for 864 ks.

Key words

Microchannel, Powder Metallurgy, Infiltration, Alkali Leaching, Nickel, Selective Leaching

1. Introduction

A metallic microreactor is suitable for catalyst reactions because it has high specific surface area and low flow resistance, which come from the microchannel structure. Additionally, it has good thermal shock resistance, high strength, and excellent heat conductivity. Some of the authors investigated the sacrificial-core method which was a simple powder-metallurgical process for producing the metallic microreactors [1-5]. In their experiments, they used two kinds of metals with different melting points: a body metal with higher melting point and a sacrificial-core metal. The body metal composes the device body, and the sacrificial-core metal gives the shape of the microchannel.

When nickel was used as the body metal and aluminum as the sacrificial-core metal, a porous thick film of Ni-Al intermetallic compounds formed as a lining layer. [4] Figure 1 depicts a Ni-Al binary alloy phase diagram. According to this diagram, the solid phase in equilibrium with Al-rich liquid changes depending on the temperature: Al₃Ni, Al₃Ni₂ and NiAl.

Catalytic activities of some Ni-Al intermetallic compounds were investigated [7-15]. Xu *et al.* reported that

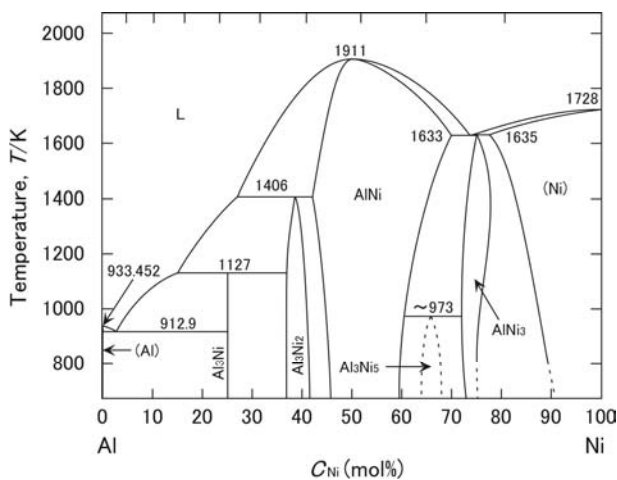


Fig. 1 Ni-Al binary alloy phase diagram based on the report by Okamoto [6]

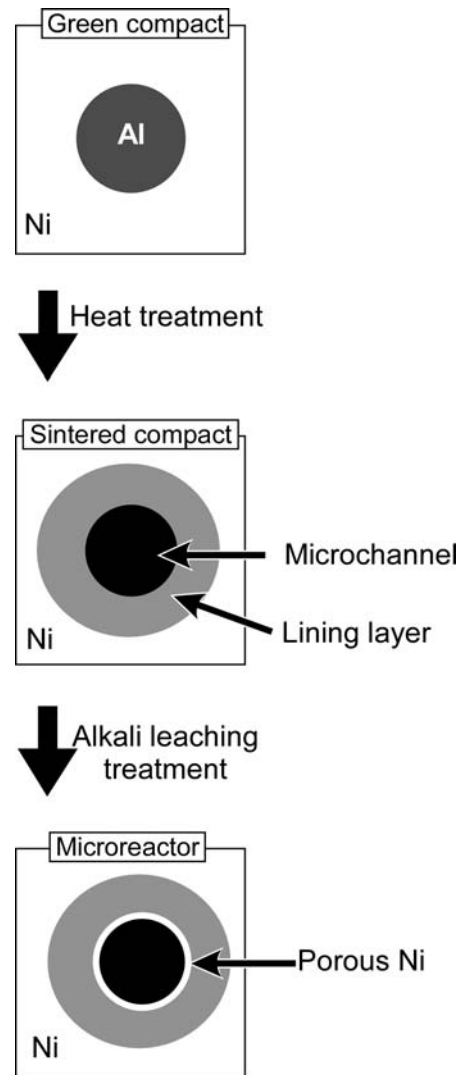


Fig. 2 Schema of the powder metallurgical microchanneling process and alkali leaching treatment of the lining layer

alkali-leached Ni_3Al powder exhibit catalytic activity for hydrogen production from methanol or methane. [7-11] A mixture of Al_3Ni and Al_3Ni_2 is well known as a precursor alloy for Raney-Ni catalysts [12-15].

In our previous study [5], we found a heat treatment condition to produce a microchannel lining layer consisting of Al_3Ni_2 , and attempted to control its composition by alkali leaching. Figure 2 illustrates the schema of our process combining the sacrificial-core method and the alkali leaching process. A green compact of nickel powder containing aluminum wire is sintered at a temperature between the melting points of these metals. During sintering of the green compact, molten aluminum migrates to the nickel powder region by infiltration and diffusion. These metals react and produce an intermetallic layer lining the microchannel formed at the sites initially occupied by the aluminum wire. Then, the lining layer is dipped in alkali solution for selective leaching of aluminum in order to give a catalytic activity to inner-wall surface of the microchannel. In our previous study, an Al_3Ni_2 microchannel lining layer was dipped in NaOH aqueous solution for 86.4 ks. As a result, the ratio of Al to Ni of the lining layer was decreased from 1.5 to 0.6, but porous Ni like Raney catalyst was not formed. Another shortcoming of our previous study was that the composition was measured only on the exposed surface of the specimens. Therefore, composition changes in the lining layer inside the microchannel were not clear.

In this study, we investigated the relationship between the alkali leaching time and the changes in the composition and structure of the Al_3Ni_2 microchannel lining layer inside the microchannel comparing with that on the specimen surface.

2. Experimental Procedure

2.1 Preparation of sintered compacts

We used 13.9 g of nickel powder and three aluminum wires as the body-metal powder and the sacrificial cores, respectively. The average diameter of the nickel powder was 5 μm . The sacrificial cores were 500 μm in diameter and 10 mm in length. The nickel powder containing the

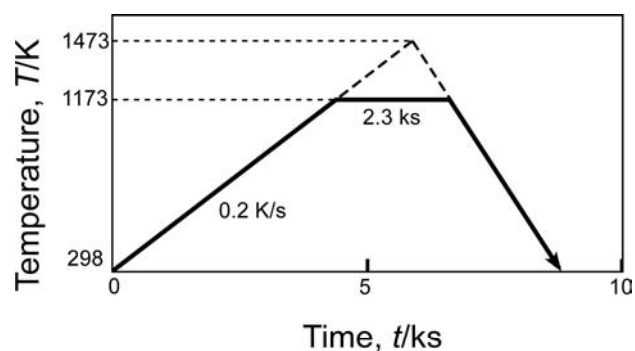


Fig. 3 Time-temperature pattern for the sintering heat treatment

sacrificial cores was cold-pressed into a cylindrical green compact in a stainless steel mold using a unidirectional pressure of 460 MPa. The shape of the resultant compact specimen was a columnar 20 mm in diameter and 5 mm in height.

The green compacts were sintered in an argon gas atmosphere. Figure 3 illustrates the time-temperature pattern during the sintering heat treatment. The broken line in Fig. 3 indicates the standard pattern used for Ni-Al microchanneling experiments in the previous study [4].

2.2 Alkali leaching treatment

The specimen after sintering was cut to thickness of 5 mm and then polished. The microchannel penetrated the specimen in the thickness direction. The specimen after polished was dipped in a NaOH aqueous solution at 323 K in order to leach aluminum. The NaOH concentration of the aqueous solution was 7 kmol/m^3 . The leaching time was varied from 0.6 to 2592 ks. The structures and compositions of the outer surface exposed to the leachant and a new surface cut after alkali leaching of the lining layer were measured by EPMA. Figure 4 shows the schema of the specimen with these surfaces. Additionally, the microstructure and composition of the inner-wall surface of the microchannel was observed by FE-SEM along with EDS.

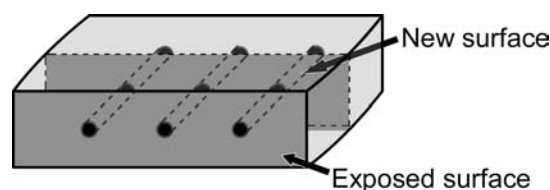


Fig. 4 Schema of the specimen

3. Results and Discussions

Figure 5 shows back-scattered electron images of the exposed surfaces before and after alkali leaching and the new surface cut after alkali leaching. The leaching time was 86.4 ks. As seen in Figs. 5 (b) and (c), many cracks formed in the lining layer by alkali leaching. No other significant changes were observed in these photographs. The average composition of the lining layer was Al-40mol%Ni before alkali leaching. The compositions measured on the exposed surface and new surface of the lining layer were changed by alkali leaching to Ni-24mol%Al-33mol%O and Ni-25mol%Al-36mol%O, respectively. This result indicated that the lining layer was dealloyed and oxidized during or after alkali leaching. The crack formation in the leached lining layer was probably caused by tensile stress resulting from deflection of aluminum.

In the experiment, the new surface cut after alkali leaching did not contact with leachant. Therefore, the surface did not oxidize during alkali leaching. In general,

Raney-Ni catalysts are very easy to oxidize because of its huge specific surface area. For this reason, Raney-Ni catalysts are preserved in water or ethanol. The oxidation of the lining layer probably occurred during the structure observation after alkali leaching due to contact with the air. Tanaka *et al.* [16] reported that Al_3Ni_2 phase was directly transformed into Ni during alkali leaching. In Fig. 5, however, the lining layer after alkali leaching had a uniform brightness which corresponded to a uniform composition. In fact, EPMA results revealed that the composition of the alkali-leached lining layer were almost uniform.

Figure 6 shows the relationships between leaching time and the ratio of Ni concentration, C_{Ni} , to Al concentration,

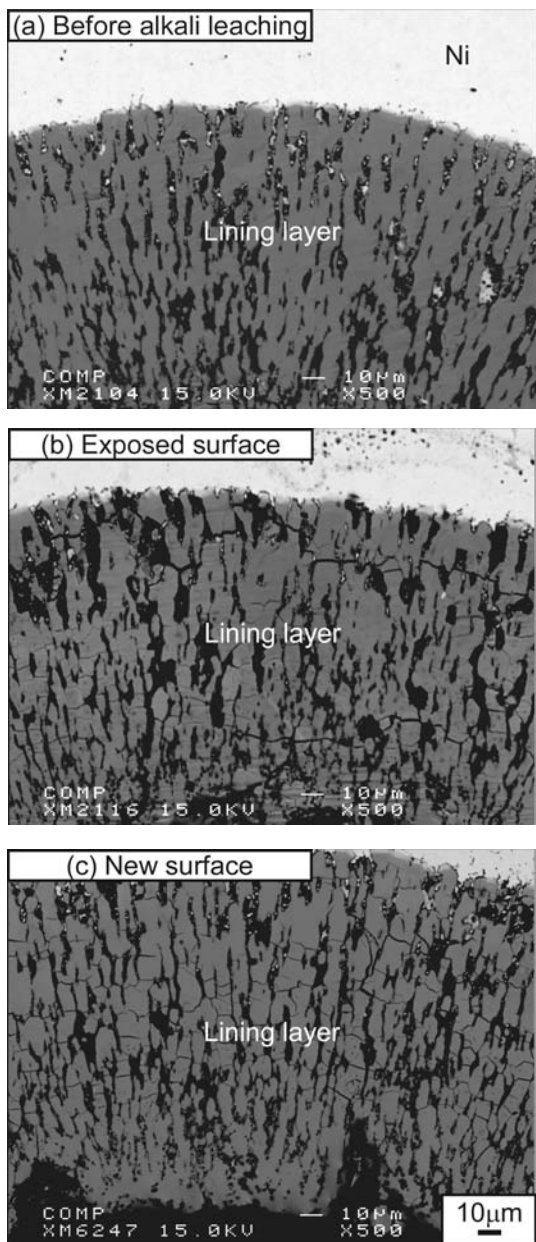


Fig. 5 Back-scattered electron images of the structures of the lining layers showing the effect of alkali leaching for 86.4ks

C_{Al} , on the exposed surface and new surface of the lining layer. The initial value of the ratio C_{Al}/C_{Ni} was 1.5 for each surface. Gray bands in Fig. 6 correspond to the composition ranges of Al_3Ni_2 , NiAl, Ni_3Al and Ni solid solution at 673K (see Fig. 1). The ratio C_{Al}/C_{Ni} on the exposed surface of the lining layer decreased to the coexistence region of NiAl and Ni_3Al until $\tau = 7.2$ ks. After $\tau = 7.2$ ks, the decrease in C_{Al}/C_{Ni} became sluggish. In the coexistence region of NiAl and Ni_3Al , the decreasing manner of C_{Al}/C_{Ni} on the new surface is similar to that on the exposed surface. Before

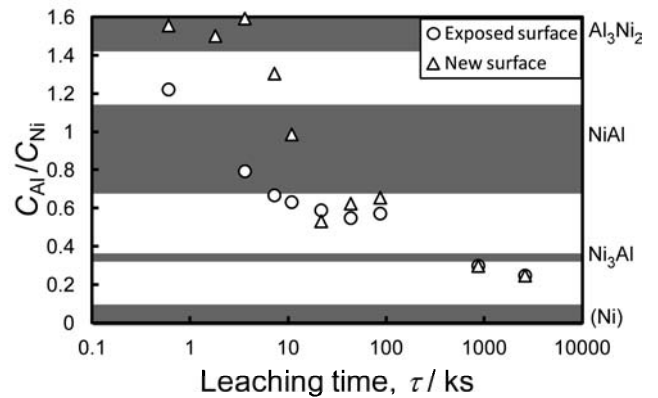


Fig. 6 Relationship between C_{Al}/C_{Ni} and the leaching time

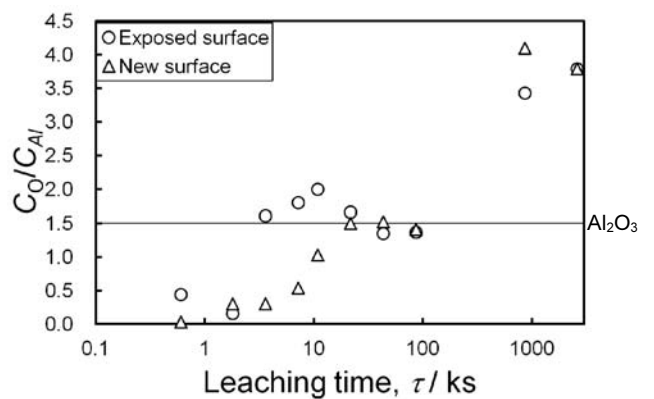


Fig. 7 Relationship between C_O/C_{Al} and the leaching time

Table 1 Relationship between C_O/C_{Al} and the elapsed time after alkali leaching

Leaching time (ks)	Time after leaching (ks)	C_O/C_{Al}
0.6	199.8	0.44
0.6	756.6	0.29
86.4	196.2	1.2
86.4	755.5	1.4

reaching the coexistence region of NiAl and Ni₃Al, C_{Al}/C_{Ni} started to decrease after $\tau = 3.6$ ks and it decreased relatively slowly compared to the exposed surface. The leachant penetrated into the long and thin pores. Therefore, the reduction of C_{Al}/C_{Ni} on the new surface started after a certain time elapsed. On both surfaces, the rate of decline of C_{Al}/C_{Ni} reduced drastically after reaching the NiAl-Ni₃Al coexistence region. Ni₃Al is known to have a very high corrosion resistance. Aluminum leaching from the lining

layer possibly became difficult due to the formation of the Ni₃Al phase.

The relationships between the leaching time and the ratio of O concentration, C_O , to C_{Al} on the exposed surface and new surface of the lining layer are shown in Fig. 7. The initial value of the ratio C_O/C_{Al} was almost 0 for each surface. The solid line in Fig. 7 indicates the index value $C_O/C_{Al} = 1.5$ which corresponds to the composition of Al₂O₃. It is noteworthy that the trend of increasing of C_O/C_{Al} on each surface in Fig. 7 corresponded to that of decreasing of C_{Al}/C_{Ni} in Fig. 6 respectively. C_O/C_{Al} on the exposed surface reached 1.5 with shorter leaching time than that on the new surface. Aluminum is oxidized preferentially compared with nickel. Therefore, oxygen detected both on the exposed and new surfaces of the lining layer probably existed in the form of Al₂O₃ in the case when τ was shorter than 86.4 ks. When τ exceeded 864 ks, both Al and Ni oxidized owing to increase in the specific surface area.

Table 1 shows the relationship between C_O/C_{Al} on the exposed surface of the lining layer and the elapsed time after alkali leaching in the air. According to this table, C_O/C_{Al} was not changed from about 200 to about 760 ks for each leaching time. This result indicates that the oxidation of the alkali-leached lining layer was not a long time process such as atmospheric corrosion of iron.

The structures of the inner wall of the microchannels before and after alkali leaching are shown in Fig. 8. A needle-like structure was observed on the inner wall of the microchannel before alkali leaching (see Fig. 8 (a)). This structure is similar to the Al₂O₃ scale produced by high-temperature oxidation of NiAl [17]. Probably, the microchannel lining layer was oxidized by air slightly remained in the compact specimen. However, this structure had been completely dissolved after alkali leaching for 0.6 ks as shown in Fig. 8 (b). After leaching for 7.2 ks, fine asperities had formed on the inner wall of the microchannel as shown in Fig. 8 (c). This result indicates that the surface area of the microchannel can be increased by alkali leaching.

Figure 9 shows the relationship between the leaching time and the composition of the inner-wall surface of the

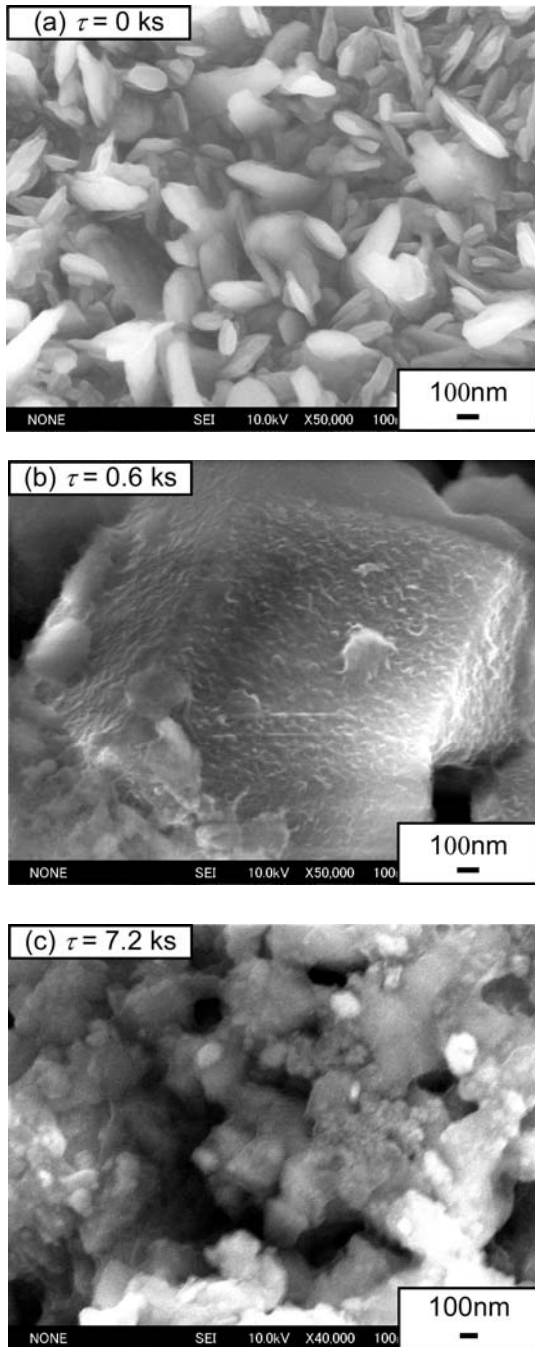


Fig. 8 Structures of the inner-wall surface of the microchannels. (a) Before alkali leaching, (b) after leaching for 0.6 ks, (c) after leaching for 7.2 ks

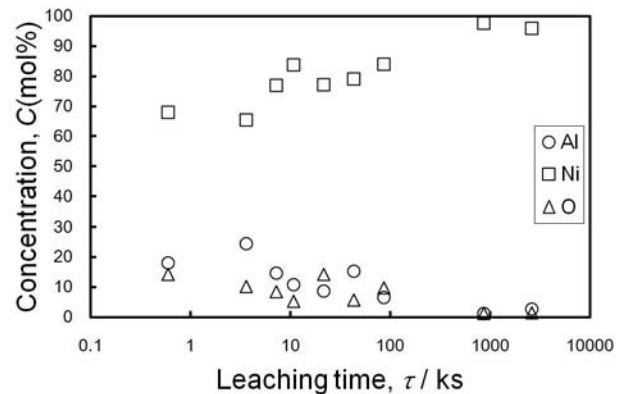


Fig. 9 Relationship between the leaching time and the composition measured by EDS on the inner-wall surface of the microchannel

microchannel. The Al, Ni and O concentrations were measured by EDS. It is noteworthy that almost pure Ni was detected on the specimen leached for 864 ks or longer. Figure 10 depicts the microstructure of the inner-wall surface of the microchannel after leaching for 864 ks. The structure has nano-scale spiny projections and it consists of almost pure Ni as we have intended in this study. This structure seems to have more orderly nature than that after 7.2 ks leaching (see Fig. 8 (c)). Possibly, reconstitution of the surface structure occurred after complete leaching, and as a result, the oxidizable nature of the surface was controlled. However, the detail mechanism is a subject for future study.

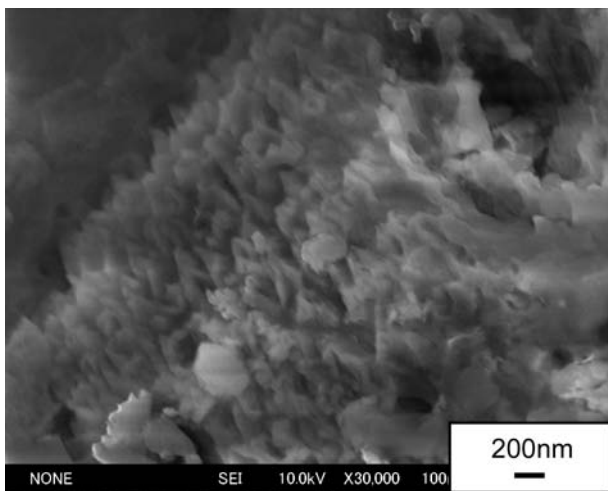


Fig. 10 Structure on the inner-wall surface of the microchannel after leaching for 864 ks

4. Conclusions

Effects of alkali leaching time on the composition and structure changes in the Al_3Ni_2 microchannel lining layer produced by the sacrificial-core method was investigated. The following conclusions were obtained.

- (1) Decrease in Al concentration become sluggish in the coexistence region of NiAl and Ni_3Al .
- (2) The lining layer after alkali leaching remarkably oxidizes due to increase in the specific surface area by the alkali leaching.
- (3) The oxidation of the alkali-leached lining layer occurs early after the lining layer contacts with air.
- (4) The needle-like structure formed on the inner-wall surface of the microchannel after sintering is dissolved by alkali leaching.
- (5) Fine asperities are formed on the inner-wall surface of the microchannel after leaching for 7.2 ks.
- (6) Almost pure Ni was detected on the inner-wall surface of the microchannel after leaching for 864 ks.

References

- [1] Ohmi, T., Kodama, T. and Iguchi, M.: Formation Mechanism of Microchannels and Lining Layers in Sintered Iron Powder Compacts with Copper Sacrificial Cores, *Mater. Trans.*, **50** (2009), 2891-2896.
- [2] Ohmi, T., Takatoo, M., Iguchi, M., Matsuura, K. and Kudoh, M.: Powder-Metallurgical Process for Producing Metallic Microchannel Devices, *Mater. Trans.*, **47** (2006), 2137-2142.
- [3] Ohmi, T., Takatoo, M. and Iguchi, M.: Powder-Metallurgical Free-Form Microchanneling Process for Producing Metallic Microreactors. *J. JSEM*, **9** (2009), 125-29.
- [4] Ohmi, T., Hayashi, N. and Iguchi, M.: Formation of Porous Intermetallic Thick Film by Ni-Al Microscopic Reactive Infiltration, *Mater. Trans.*, **49** (2008), 2723-2727.
- [5] Saitoh, Y., Ohmi, T., Sakairi, M. and Iguchi, M.: Alkali Leaching of Ni-Al Alloy Microchannel Lining Layers, *J. JSEM*, **11** (2011), SS276-SS279.
- [6] Okamoto, H.: Binary Alloy Phase Diagrams (2nd. ed., Plus Updates), *Materials Park*, (1996) (CD-ROM).
- [7] Qi, C., Amphlett, C.J. and Pepply, A.B.: Hydrogen production by methanol reforming on NiAl layered double hydroxide derived catalyst: Effect of the pretreatment of the catalyst, *Hydrogen Energy*, (2007), 5098-5102.
- [8] Xu, Y., Kameoka, S., Kishida, K., Demura, M., Tsai, P.A. and Hirano, T.: Catalytic Properties of Ni_3Al Intermetallics for Methanol Decomposition, *Mater. Trans.*, **45** (2005), 3177-3179.
- [9] Xu, Y., Kameoka, S., Kishida, K., Demura, M., Tsai, P.A. and Hirano, T.: Catalytic production from methanol, *Intermetallics*, **13** (2005), 151-155.
- [10] Xu, Y., Demura, M. and Hirano, T.: Effect of alkali leaching on the surface structure of Ni_3Al catalyst, *Applied Surface Science*, **254** (2008), 5413-5420.
- [11] Ma, Y., Xu, Y., Demura, M., Chun, H.D., Xie, G. and Hirano, T.: Catalytic activity of atomized Ni_3Al powder for hydrogen generation by methane steam reforming, *Catalysis Letters*, **112** (2006), 31-36.
- [12] Zou, J.J., Zhang, X., Kong, J. and Wang, L.: Hydrogenation of Dicyclopentadiene over amorphous nickel alloy catalyst SRNA-4, *Fuel*, **87** (2008), 3655-3659.
- [13] Lei, H., Song, Z., Tan, D., Bao, X., Mu, X., Zong, B. and Min, E.: Preparation of novel Raney-Ni catalysts and characterization by XRD, SEM and XPS, *Applied Catalysis A: General*, **214** (2001), 69-76.
- [14] Kudo, K. and Komatsu, K.: Selective formation of methane in reduction of CO_2 with water by Raney alloy catalyst, *J. Molecular Catalysis A: Chemical*, **145** (1999), 257-264.
- [15] Bakker, L.M., Young, J.D. and Wainwright, S.M.: Selective leaching of NiAl_3 and Ni_2Al_3 intermetallics to form Raney nickels, *J. Mater. Sci.*, **23** (1988), 3921-3926.
- [16] Tanaka, S., Hirose, N., Tanaki, T. and Ogata, H.Y.: Effect of Ni-Al Precursor Alloy on the Catalytic

Activity for a Raney-Ni Cathode, *J. Electrochem. Soc.*, **147** (2000), 2242-2245.

[17] Liu, G., Li, M., Zhu, M. and Zhou, Y.: Transient of alumina oxide scale on B-NiAl coated on M38G alloy at 950°C, *Intermetallics*, **15** (2007), 1285-1290.